An Onboard Navigator for the Extremely Low-Altitude Satellite Utilizing Accelerometers

Hidehiko Mori*
National Aerospace Laboratory, Tokyo, Japan

The main mission of a dive and ascent satellite flying at an extremely low altitude with perigee near 110 km is to measure the atmospheric characteristics at the bottom of the ionosphere. Continuous observation and prediction of rapidly decaying orbits is required to attain the mission of the satellite. In this paper the solutions of the Euler-Hill equations for the perturbation of orbits due to air drag are examined and compared with the simulated results obtained from the numerical integration of the rigorous differential equations. A method for approximating Jacchia's atmospheric density model by a simple function of altitude, with the exospheric temperature as a parameter, is presented. Then the least-squares estimate of air density parameters and orbital elements utilizing accelerometer data in the vicinity of the perigee is proposed for application to a small onboard computer.

Introduction

THE dive and ascent satellite (DAS) is a new aeronomy satellite flying at a very low altitude with a perigee near 110 km in the dive mode of operation.[1] NASA's Atmospheric Explorer attained the same kind of mission, but the minimum perigee altitude was about 135 km (Ref. 2). Taking the perigee altitude at 110 km poses severe problems on the satellite design, especially in heat and orbital control.

DAS has the configuration shown in Fig. 1 with solar cells mounted on the side cylinder and with a heat shield on the top to relieve thermal loads on the back part of the body. The temperature traces of four sections of the satellite are shown in Fig. 2. The figure indicates that the temperature of the solar cell is kept to a moderate degree under the protection of the heat shield. In this analysis, however, it was assumed that the symmetric axis of the satellite coincides with the direction of the velocity at perigee, and that the Earth is a sphere. In practice, the satellite is spin-stabilized, but has a slight nutation around the perigee. The direction of the velocity at perigee must vary as the perigee argument changes every revolution. Moreover, the minimum altitude of orbit does not coincide with the perigee altitude because of the nonspheric shape of the Earth. Therefore, onboard maneuverings, based on trajectory information, are required to adjust the perigee altitude and the attitude of the satellite when it stays in the neighborhood of the apogee.

The orbital decay due to air drag, most of which is encountered in a small section of the orbit near the perigee, leads to an almost 20-km decrease of the apogee altitude for each revolution. Many studies have been done on the orbital decay per revolution due to air drag, and these methods can be made applicable to trajectories with a perigee of 110 km by adjusting parameters. There are also analytic methods for obtaining the changes of other orbital elements. The orbital decay and the other orbital changes per revolution obtained from such analyses are listed in Table 1 for three cases of an apogee altitude of H_a, with the perigee altitude of 110 km unchanged.

Since the orbital decay varies largely with a daily change of the atmospheric density, continuous information concerning the air density and the orbits is required for an appropriate orbit and attitude control. Japanese tracking stations are not appropriately located for this purpose. Thus, an operational scheme which includes both ground tracking and some kind of onboard navigator is required. Since air drag is the dominant disturbing force on the satellite, accelerometers are expected to be the most efficient sensors providing input to the onboard navigator.

The analytic methods used to get the results of Table 1 can be used to predict the orbital elements in the onboard operational scheme.

Effect of Air Drag on Satellite Orbits

In the Euler-Hill equations the perturbation of satellite position from the reference Kepler motion is considered. According to the Appendix the perturbation of orbital altitude x due to air drag is expressed by the Euler-Hill equations

$$\ddot{x}+n^2x=-2B\rho_p a^2 n^2 e^{-\beta}\left[I_0(\beta)t+2\sum_{j=1}^{\infty}\frac{1}{j}I_j(\beta)\sin(jnt)\right] \tag{1}$$

where

$$\beta=k_p ae \tag{2}$$

B is the ballistic coefficient of the satellite, ρ_p the air density at the perigee altitude, n the mean angular velocity of the satellite, a the semimajor axis of the orbit, e the eccentricity of the orbit, and $I_j(\beta)$ the modified Bessel function of the jth order.

The solution of the equation corresponding to the forcing terms, which has the coefficients $I_0(\beta)$ and $I_1(\beta)$, is secular and has the form

$$x_a(t)=2B\rho_p a^2 e^{-\beta}[-I_0(\beta)nt+I_1(\beta)nt\cos nt] \tag{3}$$

The periodic solution of Eq. (1) corresponding to the remaining forcing terms is given by

$$x_p(t)=2B\rho_p a^2 e^{-\beta}\sum_{j=2}^{\infty}\frac{1}{j(j^2-1)}I_j(\beta)\sin(jnt) \tag{4}$$

The homogeneous solution for Eq. (1) is given by

$$x_H(t)=C_1\sin(nt)+C_2\cos(nt) \tag{5}$$

Presented as Paper 81-0207 at the AAS/AIAA Astrodynamics Specialist Conference, Lake Tahoe, Nev., Aug. 3-5, 1981; submitted Sept. 21, 1981; revision received Nov. 8, 1982.

*Senior Researcher.

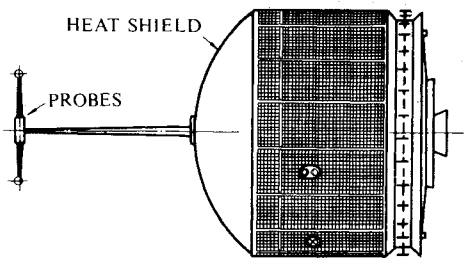

Fig. 1 External configuration of DAS.

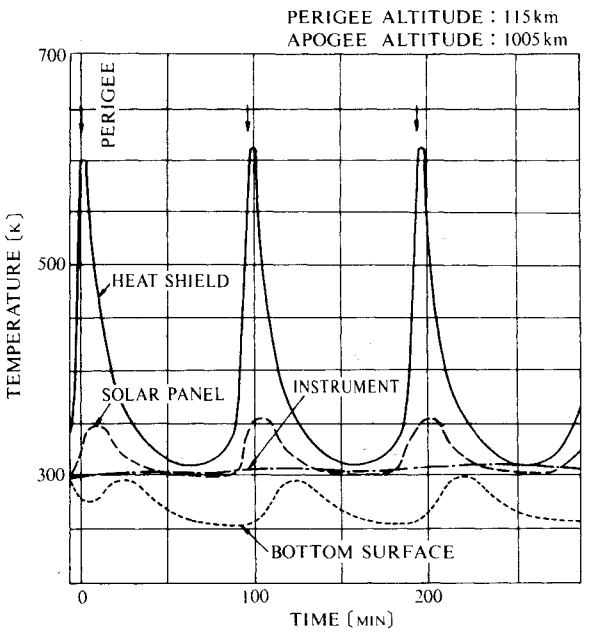

Fig. 2 Temperature traces of major components in dive mode.

Thus the complete solution of the differential equation, Eq. (1), $x(t)$ is expressed by the combination of Eqs. (3-5)

$$x(t) = x_a(t) + x_p(t) + x_H(t) \tag{6}$$

Suppose that the time when the satellite passes through perigee is the origin of time and the initial conditions are given by

$$x(0) = 0 \qquad \dot{x}(0) = 0 \tag{7}$$

Then the homogeneous solution reduces to

$$x_H(t) = K_H \sin(nt) \tag{8}$$

where

$$K_H = -2B\rho_p a^2 e^{-\beta}\left[-I_0(\beta) + I_1(\beta) + \frac{2}{3}I_2(\beta) + \frac{3}{12}I_3(\beta) + \frac{4}{30}I_4(\beta) + \cdots\right] \tag{9}$$

Table 1 Variation of DAS orbits

H_a	(km)	600	1000	2000
δ_a	(km/rev)	−26.29	−19.20	−17.77
δH_p	(km/rev)	−0.2862	−0.1171	−0.0372
$\delta\Omega$	(deg/rev)	−0.1798	−0.1705	−0.1520
$\delta\omega$	(deg/rev)	−0.1090	−0.1031	−0.0908
δi	(deg/rev)	0.00431	0.00346	0.00284

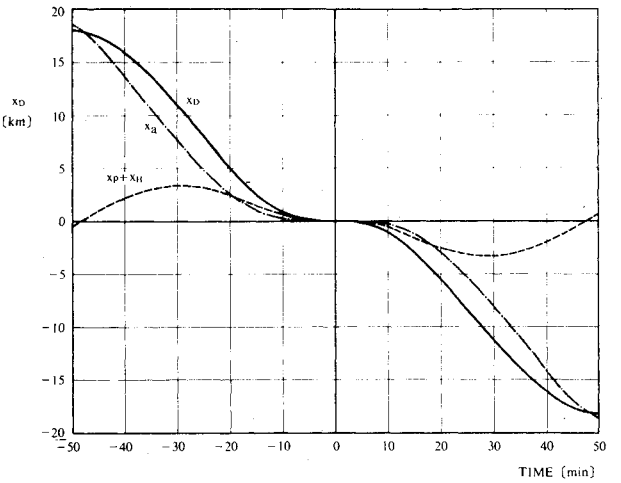

Fig. 3 Contribution of each term in Eq. (9).

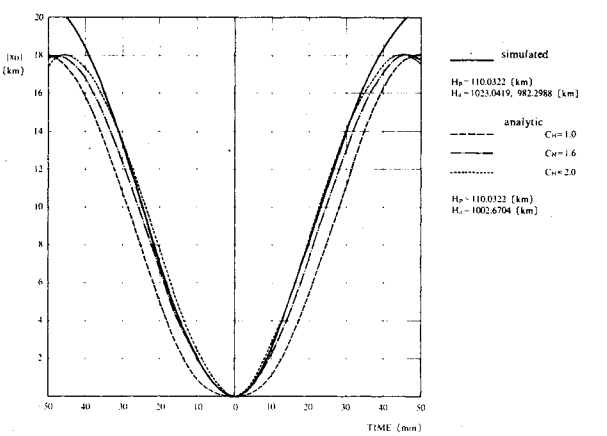

Fig. 4 Comparison of the analytic solution and the simulated results for the perturbation of air drag.

In the derivation of Eq. (6) we used the assumption of a spheric Earth. In practice, however, the minimum altitude of orbit does not coincide with the perigee altitude of the nominal Kepler motion because of the variation of the Earth radius and the perturbation of orbit due to the oblateness of the Earth. The initial conditions, Eq. (7), should be given for time at minimum altitude $t = t_m$ in order to take into account the oblate shape of the Earth. Therefore, the solution of Eq. (1) for the oblate Earth, x_D, is expressed approximately as

$$x_D(t) = x_a(t - t_m) + x_p(t - t_m) + x_H(t - t_m) \tag{10}$$

For $j \geq 2$, $I_j(\beta)$ is reduced to the form including only $I_0(\beta)$ and $I_1(\beta)$, using the relation

$$I_j(\beta) = I_{j-1}(\beta) + (2j/\beta) I_j(\beta)$$

and $I_0(\beta)$ and $I_1(\beta)$ are expressed in the asymptotic series

$$e^{-\beta} I_0(\beta) = \frac{1}{(2\pi\beta)^{1/2}}\left[1 + \frac{1^2}{1!(8\beta)} + \frac{1^2 \cdot 3^2}{2!(8\beta)^2} + \cdots\right]$$

$$e^{-\beta} I_1(\beta) = \frac{1}{(2\pi\beta)^{1/2}}\left[1 - \frac{1 \cdot 3}{1!(8\beta)} - \frac{1^2 \cdot 3 \cdot 5}{2!(8\beta)^2} - \cdots\right]$$

The reference trajectory of DAS is given by $H_p = 110$ km, $H_a = 1000$ km, $i = 70$ deg, and $\omega = 30$ deg. The time history of each term in Eq. (9) is shown in Fig. 3 for nearly one revolution. Time at minimum altitude t_m was taken to be −0.45 min.

This analytic solution $x_D(t)$ is compared with the solution obtained from the trajectory simulation. One of the results is

shown in Fig. 4. In the simulation, the effect of air drag and the variation of the Earth's radius due to its nonspheric shape were included, but the effect of the Earth's oblateness on the gravity potential was neglected. The computation of the trajectory was started at perigee with the osculating elements $H_p = 110.6$ km, $H_a = 1115.0$ km, $i = 70$ deg, and $\omega = 30$ deg.

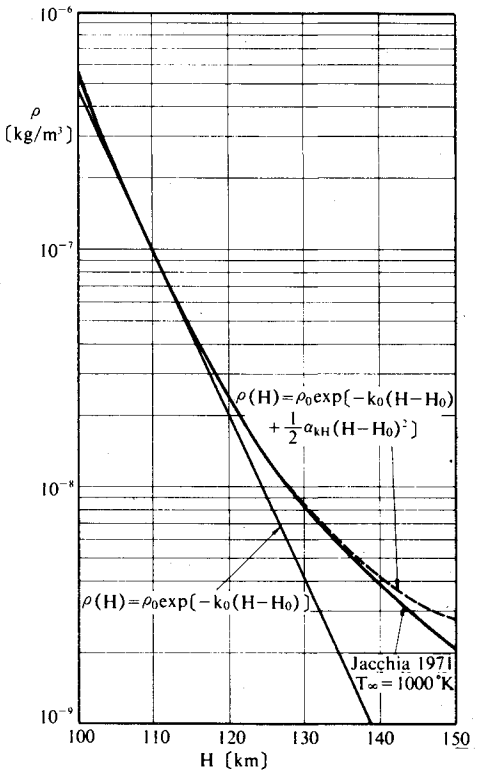

Fig. 5 The approximation of the air density.

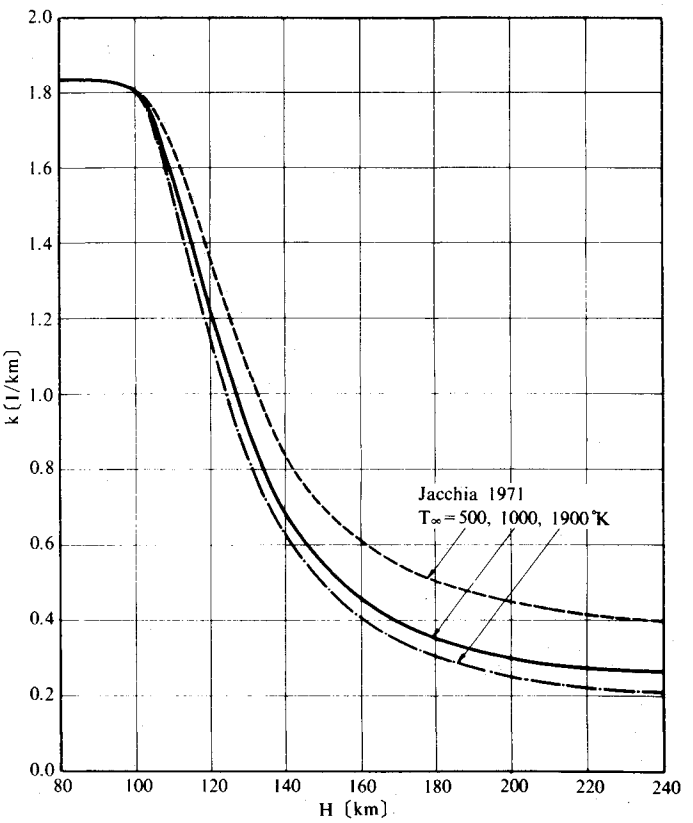

Fig. 6 The variation of k according to the altitude and exospheric temperature.

Figure 4 shows the result of the third revolution. The perigee altitude of the nominal Kepler motion was taken to be the same as the simulated perigee altitude and the apogee altitude of the Kepler motion was supposed to be the mean of the third and the fourth apogee altitude in the simulation.

The analytic solution is shown in a broken line labeled $C_H = 1.0$. Near the starting point of the simulation from perigee the approximation was good, but the approximation for the third revolution shown in the figure is not good. When a satellite approaches perigee from apogee, the perturbational velocity $\dot{x}_D(t_m)$ differs slightly from zero. The inadequate initial conditions of Eq. (7) caused the error. In order to adjust the initial value $\dot{x}_D(t_m)$, we multiplied Eq. (9) bya coefficient C_H. Then for $C_H = 1.0$, both $x_D(t_m)$ and $\dot{x}_D(t_m)$ are zero. For $C_H \neq 1.0$, $x_D(t_m)$ is zero, but $\dot{x}_D(t_m)$ can havea nonzero value. For the case shshown in Fig. 4, simulated $\dot{x}_D(t_m)$ was -1.666 m/s, while $\dot{x}_D(t_m)s$ for the analytic solutions shown in Fig. 4 were -1.865 m/s for $C_H = 1.6$ and -3.108 m/s for $C_H = 2.0$. The analytic solution can be brought close enough to the simulated result by adjusting the value of C_H, though the same $\dot{x}_D(t_m)$ as the simulated solution does not necessarily give the best approximation. If the region is limited to only ± 10 min around the perigee, the approximation shows good improvement.

Air Density Model

In the derivation of the analytic solution of the perturbation of air drag, the air density was supposed to be $\rho(H) = \rho_p \exp[-k_p(H - H_p)]$. This approximate model, with the perigee altitude of 110 km, is compared with the air

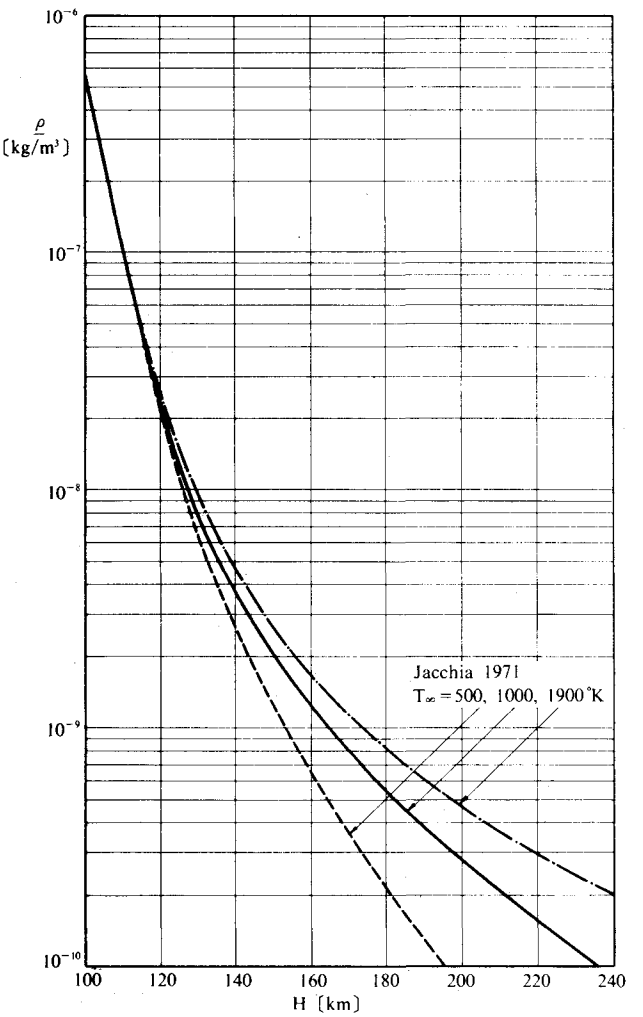

Fig. 7 The variation of air density according to the altitude and the exospheric temperature.

density model used for the trajectory simulation in Fig. 5. Such a model may be used for obtaining an analytic expression of the decaying orbit, but is not appropriate for estimating the air density, or orbital elements in the vicinity of perigee, from the accelerometer data. An elaborate air density model has been proposed by Jacchia.[4] In the following, a simplified expression of Jacchia's model below 200 km is investigated for application to an onboard navigator.

The exospheric temperature at a given time and position on the Earth can be analytically determined if the solar flax $F_{10.7}$ and the planetary geomagnetic index K_P are given by meteorological observation. The basic air density at an altitude for an exospheric temperature is calculated by integrating the air density in the lower region. This calculation is very tedious, but the results are shown in the basic table of Jacchia's paper.[4] Some results of special interest are plotted in Figs. 6 and 7. It is not difficult to generate the air density for a given altitude and a given exospheric temperature to the desired degree of accuracy by the interpolation of stored basic data in an onboard computer. Suitable fitting functions for $\rho(H)$ and $k(H)$ below 200-km altitude are given by

$$k(H)=k_j-\alpha_j(H-H_j) \tag{11}$$

and

$$\rho(H)=\rho_j\exp[-k_j(H-H_j)+(\alpha_j/2)(H-H_j)^2] \tag{12}$$

where j indicates the jth data of the basic table for a given exospheric temperature, and α_j is the slope of $k(H)$ at $H=H_j$ in Fig. 7. $k(H)$, in the neighborhood of 110 km, is approximated exceptionally well by Eq. (11). The relation required for k and ρ, $k=-(\partial\rho/\partial H)/\rho$, is continuously satisfied by Eqs. (11) and (12). As a result, $\rho(H)$, expressed by Eq. (12), approximates the basic air density well in the region where the approximation of Eq. (11) is effective. The result of the formulas applied to the case $T_\infty=1000$ deg at $H_j=110$ km is shown in Fig. 5. The basic density is well approximated between 105 and 125 km. Applying these formulas to several data points, we can get an approximate expression for the basic air density below 200-km altitude.

In order to get the actual air density below 200 km, some correction terms have to be added to the basic density. These are the effects of the planetary geomagnetic index variation and the seasonal-latitudinal variations of the lower thermosphere. The corrections for both of these variations are expressed in the form $\Delta\log\rho$, and the corrected air density is given by

$$\bar{\rho}=(1+\ell n10\Delta\log\rho)\rho \tag{13}$$

The effect of the planetary geomagnetic index variation does not depend on the altitude. Thus the correction is easily done simultaneously with the correction of the exospheric temperature every day. On the other hand, the effect of the seasonal-latitudinal variations of the lower thermosphere varies according to the altitude, the latitude and the season, though the magnitude of the variation is small. Since the mission period is limited to a short time, the seasonal variation can be neglected. The latitudinal variation can be compensated for by the correction factor obtained from Eq. (13). This variation is evaluated only for the latitude of the perigee. In order to compensate for the variation due to altitude, $\rho(H)$ and $k(H)$ must be multiplied by functions of H obtained from Jacchia's correction formula. These corrections can be applied to the basic data before applying Eqs. (11) and (12), and the actual density must be expressed by these equations for the corrected data.

The air drag per unit mass of a satellite is given by

$$D=B\rho v^2 \tag{14}$$

Substituting Eq. (14) into Eq. (9) and solving for $H-H_j$, we get

$$H-H_j=k_j/\alpha_j-\sqrt{(k_j/\alpha_j)^2+(2/\alpha_j)\ell n[D/(B\rho_j v^2)]} \tag{15}$$

The velocity of the satellite relative to the air which is supposed to rotate with the Earth is approximated in the neighborhood of the perigee by

$$v\simeq\sqrt{(\mu/a)(1+e)/(1-e)}-\omega_e r\cos i \tag{16}$$

where ω_e is the Earth's rotational velocity. Thus Eq. (15) can be used to get the altitude H from the drag D measured by accelerometers if the ballistic coefficient and the air density, or their product, are known. In practice, however, neither the calculations of the air density nor the ballistic coefficient are accurate enough at an altitude below 200 km, because of the lack of measured data. Therefore, measuring the air density is itself an important mission of this satellite.

Expression of Altitude Near Perigee

The altitude of orbit H can be approximated by

$$H=r-R_L+x_z+x_D \tag{17}$$

where r is the orbital radius of the reference Kepler motion, R_L is the Earth radius as a function of the latitude L, and x_z is the perturbation of the orbit due to the second zonal term of the Earth's gravity potential in the direction of the orbital radius. x_D is given by Eq. (6). The terms of the right-hand side are expressed analytically as follows.

$$r=a(1-e^2)/(1+e\cos\theta^*) \tag{18}$$

$$R_L=R_e(K_1+K_2\cos2L-K_3\cos4L) \tag{19}$$

$$x_z=(J_2R_e^2/2a)[1-(3/2)\sin^2 i\cos2\theta] \tag{20}$$

$$\begin{aligned}x_D=2B\rho_m a^2[&-EI_0(\beta)\theta_m+EI_1(\beta)\theta_m\cos\theta_m\\&+(1/3)EI_2(\beta)\sin2\theta_m+(1/12)EI_3(\beta)\sin3\theta_m+\cdots\\&-C_H\{-EI_0(\beta)+EI_1(\beta)+(2/3)EI_2(\beta)\\&+(1/4)EI_3(\beta)+\cdots\}\sin\theta_m]\end{aligned} \tag{21}$$

The deviation angle of orbit between the minimum altitude and the perigee θ_m is given by

$$\theta_m=\theta^*-\theta_m^* \tag{22}$$

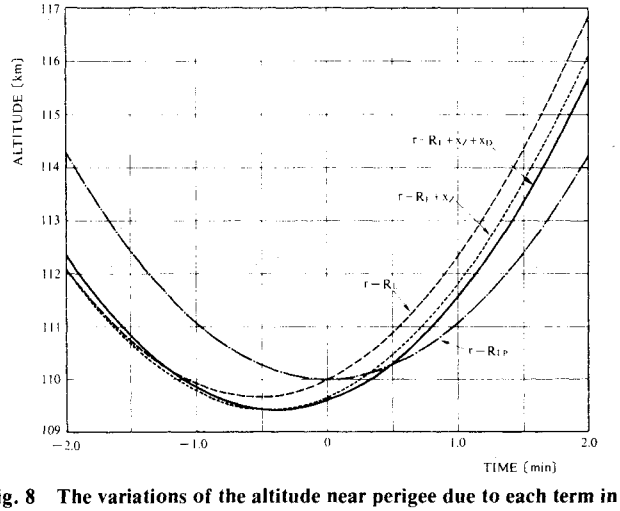

Fig. 8 The variations of the altitude near perigee due to each term in Eq. (17).

where the minimum altitude H_m and θ_m^* has the relation

$$H_m = H(\theta_m^*) = \min_{\theta^*} (r + x_z - R_L) \tag{23}$$

In these expressions, θ^* is the true anomaly, R_e is the Earth radius at the equator, and K_1, K_2, and K_3 are constants to express the nonspheric shape of the Earth. $EI_j(\beta)$ stands for $\exp(-\beta) I_j(\beta)$.

The contribution of each term in Eq. (17) for the reference trajectory of DAS is shown in Fig. 8. R_{Lp} is the Earth radius at the latitude of perigee and $r - R_{Lp}$ is the altitude of the reference Kepler motion for which the Earth radius is fixed at R_{Lp}. The minimum altitude is about 0.7 km lower than the perigee altitude, and the time of the minimum altitude deviates in this case, from the time of perigee by -0.45 min.

The gradient relating air density to altitude is so steep that the time of the minimum altitude t_m can be detected by accelerometers with good accuracy. The reference Kepler motion is defined for an orbit from one apogee to the next. And the semimajor axis a can be approximated by

$$a = \frac{1}{2}\left(\frac{\mu}{2\pi}\right)^{2/3} [(t_m - t_m')^{2/3} + (t_m' - t_m'')^{2/3}] \tag{24}$$

Table 2 Nominal values of parameters

Air density parameters	Orbital elements
$\rho_p = 99.37$ kg/km^3	$a = 6928.47$ km
$k_p = 0.1580$ l/km	$r_p = 6483.47$ km
$\alpha_p = 0.0035$ l/km^2	$t_p = 0.0$ min
$C_H = 1.7$	$\omega = 30.0$ deg

Table 3 Cases examined in least-squares estimate

Cases	Estimated parameters	Condition No. of A	No. of A'
I	8 parameters	$>10^{21}$	0.104×10^{18}
II	4 air density parameters	0.224×10^{6}	0.286×10^{2}
III	4 orbital elements	0.166×10^{11}	0.342×10^{8}

Table 4 Assumed errors in parameters

Air density parameters	Orbital elements
$\epsilon\rho_p = 0.9937$ kg/km^3	$\epsilon a = 2.0$ km
$\epsilon k_p = 0.00158$ l/km	$\epsilon r_p = 0.1$ km
$\epsilon\alpha_p = 0.35 \times 10^{-4}$ l/km^2	$\epsilon t_p = 0.01667$ min
$\epsilon C_H = 0.17$	$\epsilon\omega = 0.001745$ rad

where t_m'', t_m', and t_m are the sequential times of the minimum altitude. If a, r_p, and ω are predicted by the ground station, or by other means, θ_m^* can be calculated by Eqs. (22) and (23). The time of perigee of the reference Kepler motion is given by

$$t_p = t_m - \frac{1}{n(1+2e)}\theta_m^* \tag{25}$$

Least-Squares Estimate

The relation between air drag and the parameters to be estimated are stated in the preceding sections. There are eight parameters to be estimated—$B\rho_p$, k_p, α_p, C_H, a, r_p, t_p, and ω. B and ρ_p always appear in a combined form, and there is no need for a separate estimate. Therefore, $B\rho_p$ is dealt with as one parameter and, for convenience, its error is represented by ρ_p in the following analysis. The nominal values of the eight parameters are listed in Table 2.

Let the observation at time t_i be $y_M(t_i)$ and its prediction be $y_c(\xi, t_i)$. ξ is a vector whose elements are composed of parameters to be estimated. The least-squares estimate of parameter ξ is given as the difference $\Delta\xi$ from the predicted value ξ_0 by

$$A^T A \Delta\xi = A^T z(\xi) \tag{26}$$

where A is a matrix whose column is a vector $\partial y_c(\xi, t_i)/\partial\xi$ $(i = 1,2,\ldots,n)$ and $z(\xi)$ is a row vector, the elements of which are given by

$$z_i(\xi) = y_M(t_i) - y_c(\xi, t_i) \qquad (i = 1,2,\ldots,n) \tag{27}$$

In order to get an estimate, time sequential data have to be sufficiently independent. The condition number of A (the ratio of the moduli of the largest and smallest eigenvalue of $A^T A$) is considered as an index of the necessary figures of computation. Adopting a scale change of every ξ_j, we can transform $A^T A$ into $A'^T A'$ so that every diagonal element of $A'^T A'$ becomes unity. As a result, the figures required to compute the transformed equation

$$A'^T A' \Delta\xi = A'^T z(\xi) \tag{28}$$

can be reduced. We examined the condition numbers of both A and A' and actually solved Eqs. (26) and (28) for several cases.

First, the drag measured by accelerometers was assumed as the measured data $y_M(t_i)$. $y_c(\xi, t_i)$ is the analytic formula given by Eqs. (12) and (14) in which the perigee altitude H_p is taken to be a reference point

$$D = B\rho_p v^2 \exp[-k_p(H_i - H_p) + \tfrac{1}{2}\alpha_p (H_i - H_p)^2] \tag{29}$$

Table 5 Orbital element error effects on the estimation of air density parameters

	ϵa	ϵr_p	ϵt_p	$\epsilon\omega$
$\Delta\rho_p$	0.408 D−1	0.158 D+1	0.344 D−1	0.363 D+0
Δk_p	−0.598 D−3	0.393 D−3	−0.411 D−4	−0.116 D−3
$\Delta\alpha_p$	0.253 D−4	−0.172 D−5	0.272 D−5	−0.864 D−6
ΔC_H	−0.147 D−1	0.105 D−2	−0.167 D+0	0.103 D−1

Table 6 Air density parameter error effects on the estimation of orbital elements

	$\epsilon\rho_p$	ϵk_p	$\epsilon\alpha_p$	ϵC_H
Δa	0.231 D+0	−0.941 D+0	−0.231 D+1	0.879 D−1
Δr_p	0.235 D+0	−0.128 D+1	0.713 D+0	0.592 D−2
Δt_p	−0.757 D−2	0.559 D−1	−0.289 D−1	−0.172 D−1
$\Delta\omega$	−0.130 D−1	0.961 D−1	−0.532 D−1	−0.236 D−3

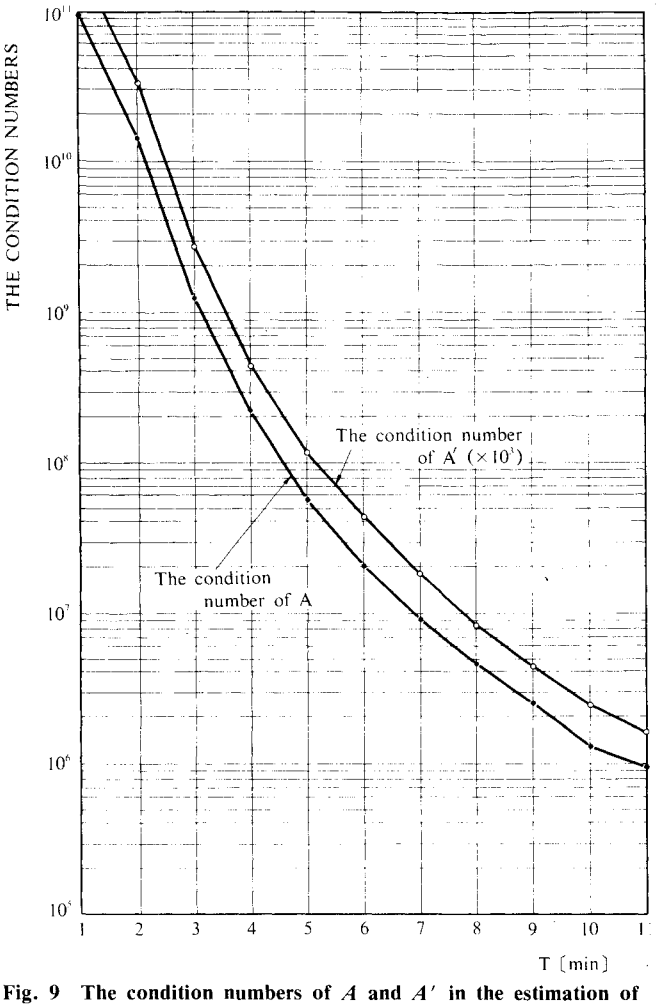

Fig. 9 The condition numbers of A and A' in the estimation of orbital elements.

The altitude H_i at an observation time t_i is given by Eqs. (17)-(23). Equation (29) is effective only for an altitude from 105 to 125 km, where the equation holds to a good approximation. The altitude for ± 2 min around perigee stays in this region, as shown in Fig. 8. Thus the data were assumed to be composed of time sequential measurements involved in ± 2 min around perigee. The three cases listed in Table 3 were examined. When all eight parameters were included, the condition number was a 17-digit number even for A'. Only 18.3 significant figures can be computed in the double-precision mode of the FACOM 230 66/75 computer. Though the significant figures are close to the condition number, Eq. (28) could not be solved by this computer.

In the second case, four air density parameters ρ_p, k_p, α_p, and C_H were chosen as the parameters to be estimated, assuming the four orbital elements to be given. The condition numbers were so small that Eq. (28) was solved by single precision computation with 7.8 significant figures of the computer. In this computation the orbital elements were assumed to have been predicted by other methods such as ground tracking. And the effects of the error in prediction were evaluated by inserting assumed errors in Eq. (28). Assumed errors in orbital elements ϵa, ϵr_p, ϵt_p, and $\epsilon\omega$ are listed on the right side of Table 4. The resultant errors in the estimation of the air density parameters $\Delta\rho_p$, Δk_p, $\Delta\alpha_p$, and ΔC_H are listed in Table 5.

Conversely four air density parameters were assumed to be given and four orbital elements were estimated by Eq. (28) in case III. Assumed errors in the air density parameters are on the left side of Table 4 and the resultant errors in the orbital elements are shown in Table 6.

In order to evaluate the methods, the assumed errors in Table 4 should have been replaced by 3σ errors in other prediction methods. If the resultant estimates of Table 4 or Table 5 were smaller than the corresponding 3σ errors, then we could say the estimates were effective. Unfortunately, we do not have such data at hand. The supposed errors in Table 4 were taken as provable values in consideration of the results of preceding sections. If the 3σ errors in other prediction methods have close values to the ones of Table 4, the estimate of the air density parameters is regarded as reasonable, but the estimate of orbital elements as poor.

For the estimate of orbital elements it is better to use data obtained from a longer time period. Thus we try to extend the data area for the estimate of case III. Equation (29) is effective only for $105 \leq H \leq 125$ km, and is not used as $y_c(\xi, t_i)$ for this purpose. The altitude H calculated from Eq. (15) utilizing accelerometer data can be used as measured quantity $y_M(t_i)$, and ρ_i, k_i, α_i $(i=1,2,...)$, and C_H are assumed to be given in this case. Inevitably, Eq. (15) is regarded as the predicting function $y_c(t_i, \xi)$.

The condition numbers of A and A' are decreased as the period of observation is increased. Figure 9 shows their variations according to the data area $2T$, which means $\pm T$ min around perigee. The approximation of Eq. (15) is expected to have a good accuracy below the altitude of 200 km. Therefore, $T=8$ min at which the altitude attains about 190 km is appropriate for this estimation. For $T=8$ min the condition numbers of A and A' are 4.6×10^6 and 8.2×10^3. Therefore, the single precision of computation with 7.8 significant digits was enough to solve Eq. (28).

In this estimation, the errors in prediction, not only in ρ_p, k_p, α_p, and C_H, but also in ρ_i, k_i, and α_i, necessary to represent the air density up to 200 km affect the accuracy of the orbital elements. If the errors are distributed randomly with moderate magnitudes, the estimated results will become better than those of Table 6.

There are two ways of getting matrix A—numerical and analytic. The numerical method is not desirable for onboard computation because the necessary figures to calculate the column of A, $\partial y_c/\partial\xi_j$, may amount to as many as ten digits. It is not difficult to derive the analytic formula for $\partial y_c/\partial\xi_j$ $(j=1,2,...,m)$ from the relations Eqs. (17-23), and they give A to a reasonable accuracy by the single precision of computation with 7.8 digits.

Conclusion

An onboard navigator utilizing a small computer and accelerometers can be set up for the dive mode of DAS mission. The estimations are conducted, with the aid of ground tracking, combining the following two procedures.

1) The air density parameters at perigee describe the air density for altitudes from 105 to 125 km. They are determined by a 32-bit onboard computer, utilizing accelerometer data obtained from 2 min before to 2 min after the perigee, if the orbital elements are predicted to a reasonable accuracy.

2) The orbital elements a, r_p, t_p, and ω of the reference Kepler motion can be estimated by a 32-bit onboard computer, utilizing accelerometer data from 8 min before to 8 min after the perigee, if the air density parameters below 200 km are given to a reasonable accuracy.

Appendix: Perturbational Equation in Altitude for the Air Drag

The air drag D per unit mass of a satellite is given by

$$D = B\rho v^2 \tag{A1}$$

where $B = C_D S/2m$ is a ballistic coefficient of the satellite of mass m, drag coefficient C_D, and reference area S. ρ_p is the air density and v is the velocity of the satellite. In order to obtain an analytic solution, we assume that the air density ρ at altitude H is expressed by

$$\rho(H) = \rho_p \exp[-k_p(H-H_p)] \tag{A2}$$

where ρ_p is the air density at the perigee altitude H_p, and k_p the inverse of a scale height.

For a Keplerian orbit, H and H_p are given by

$$H+R_e=a(1-e\cos E) \quad \text{and} \quad H_p+R_e=a(1-e)$$

where R_e is the Earth radius, a the semimajor axis, e the eccentricity, and E the eccentric anomaly of the orbit. From the last two equations,

$$H-H_p=ae(1-\cos E)$$

Substitution of this relation into Eq. (A2), with $\beta=k_p ae$, gives

$$\rho(H)=\rho_p \exp(-\beta+\beta\cos E) \tag{A3}$$

On expanding Eq. (A3) as a power series in modified Bessel functions $I_j(\beta)$, we have

$$\rho(H)=\rho_p e^{-\beta}\left[I_0(\beta)+2\sum_{j=1}^{\infty} I_j(\beta)\cos(jE)\right] \tag{A4}$$

For nearly circular orbits, E is approximated by the mean motion nt and v by the circular velocity $\sqrt{a/\mu}$. Employing these approximations, we get the expression for the air drag D from Eqs. (A1) and (A4).

$$D=B\rho_p n^2 a^2 e^{-\beta}\left[I_0(\beta)+2\sum_{j=1}^{\infty} I_j(\beta)\cos(jnt)\right] \tag{A5}$$

The perturbational effect of air drag on a satellite orbit is described by the Euler Hill equations

$$\ddot{x}-2n\dot{y}-3nx=0 \tag{A6}$$

$$\ddot{y}+2n\dot{x}=-D \tag{A7}$$

where x is the perturbation of orbital position in the direction of the orbital radius and y in the progressing direction of the orbit perpendicular to x direction. Integrating Eq. (A7) and substituting it into Eq. (A6), we obtain the perturbational equation in altitude for the air drag

$$\ddot{x}+n^2x=-2B\rho_p n^2 a^2 e^{-\beta}\left[I_0(\beta)t+2\sum_{j=1}^{\infty}\frac{1}{j}I_j(\beta)\sin(jnt)\right] \tag{A8}$$

The above derivations of equations are from Ref. 3.

References

[1] Godai, T. and Nagasu, H., "The Dive and Ascent Satellite Program for Lower Ionosphere Research," *Acta Astronautica,* Vol. 6, pp. 1409-1431.

[2] Fuchs, A.J. and Velez, C.E., "Ground Control of Drag Satellite Utilizing Onboard Accelerometer Drag," *Journal of Spacecraft and Rockets,* Vol. 13, March 1976, pp.

[3] Breakwell, J.V., Class Notes of Space Mechanics, Stanford University, May 1974.

[4] Jacchia, L.G., "Revised Static Models of the Thermosphere and Exosphere with Empirical Temperature Profiles," SAO Special Rept. 332, May 1971.

[5] King-Hele, D.G., "Methods of Determining Air Density from Satellite Orbits," *Annales de Geo Physique,* Vol. 22, No. 1, Jan.-March 1966, pp.

[6] Rugge, H.R. and Ching, B.K., "Atmospheric Density from the Low Altitude Satellite 1970-48A: Comparison of Orbital Decay Measurements and Atmospheric Models," *Planetary Space Science,* Vol. 23, 1975, pp. 323-335.